Available online www.jocpr.com

Journal of Chemical and Pharmaceutical Research, 2015, 7(4):1175-1186

Research Article

ISSN : 0975-7384
CODEN(USA) : JCPRC5

Structural and electrochemical study of binary copper alloys corrosion in 3% NaCl solution

Laidi Babouri[1], Kamel Belmokre[1], Abdenour Kabir[1], Abdesselam Abdelouas[2] and Yassine El Mendili*[2]

[1]Departement des sciences de la matière, faculté des sciences,Université du 20 aout 1955-Skikda, Algérie
[2]SUBATECH, CNRS-IN2P3, Ecole des Mines de Nantes-Université de Nantes, 4 rue Alfred Kastler, BP 20722, 44307 Nantes cedex 03, France

---

ABSTRACT

The interaction of binary copper alloys with aggressive environment may results in the formation of an adhering and protective film with time. In the present study, we investigated the corrosion of the Cu-Zn (brass) and Cu-Ni (cupronickel) alloys in 3% NaCl environment to simulate the sea waterdesalinationplants conditions. Alloys corrosion was investigated by electrochemical tests and weights loss measurements. The morphology and the nature of corrosion products formed at open circuit potential in 3% NaCl solution were analyzed using scanning electron microscopy and confocal micro-Raman spectroscopy. The results show the formation of Cu_2O, CuO, $Cu_3Zn(OH)_6Cl_2$ and ZnO for the brass, while for the cupronickel, the corrosion products show the incorporation of nickel in the corrosion products (Cu_2O, CuO, $Cu_3Ni(OH)_6Cl_2$ and NiO), which reduce the denickelisation of Cu-Ni alloy. Our results clearly show that the copper-nickel alloy is more resistant towards corrosion in NaCl environment than copper-zinc alloy.

Keywords: Copper alloys, 3% NaCl, corrosion, electrochemical techniques, structural characterisation.

INTRODUCTION

Pure copper is rarely used as a corrosion resistant material within the marine environment. Copper-based alloys, however, such as the copper nickel, aluminum and zinc, have an extensive range of marine applications. The corrosion of copper and its alloys has been widely studied in chloride media where it has been observed that the chloride ion has a strong influence on the copper corrosion mechanism **[1].**

Binary alloys of copperare widely used in industry, mainly in the seawater desalination plants, due to their outstanding physical and mechanical properties **[2]**. However, these materials are not thermodynamically stable and are vulnerable to corrosion in contact with an aggressive environment **[3]**. The result of their interactions is the loss of some or all of their essential properties. They may also be subject to some form of corrosion such a spitting corrosion and/or selective dissolution **[4-6]**.

The surface degradation of copper alloys results in the formation of an oxide film and/or adhering hydroxide which limits the transport of metal ions of the layers interacting with the medium that promoting the protection of the metal surface **[7]**.

Most studies on binary alloys of copper are focused on understanding the passive film formation mechanism **[8],** its quality **[9],** the influence of some experimental conditions (pH, the applied potential, the polarization time and the presence of aggressive anions) on its stability **[10-15]**, it sticknesse and its composition **[16,17].**

Previous studies showed a selective dissolution of brass in chloride environment and concluded that chloride promotes the dissolution of both copper and zinc **[18-20]**.

The Cu-Ni alloys constitute one of the most appealing Cu-based alloys due to their superior and tuneable mechanical properties as well as outstanding corrosion resistance. They have been used for many years in seawater, where they offer high resistance against bio-fouling **[21]**.

The aim of the present work was to study the corrosion behavior of α-phase for bothCu-Zn and Cu-Ni alloysin chloride-rich environment with application in the field of sea water desalination and power generation in Algeria. Electrochemical tests, weight loss measurements combined with structural studies of the corrosion films were conducted to describe the stability of alloys in aggressive chloride-rich environments.

EXPERIMENTAL SECTION

Copper alloys preparation

The materials used inthis study are a Cu_Ni and Cu_Zn alloys, provided bythe Skikda power plant (Algeria) and made by *SNC-Lavalin* Group Inc (Canada). These alloys are used for a wide range of applications including manufacturing of boilers, pressure vessel and pipes transporting hot liquids. The chemical composition of Cu-Zn and Cu-Ni alloys, obtained by EDX spectroscopy are given in **Table 1**.

The samples coupons were cut into 15 × 15 × 0.8 mm^3 and polished with a Buehler polisher using a PSA discs (Pressure Sensitive Adhesive discs) to a surface roughness of 0.3 microns.

Table 1: Elementalchemicalcomposition of Cu-Zn and Cu-Ni alloys (in atomic %)

Alloys	composition (%)						
	Cu	Ni	Zn	Al	Fe	Co	Mn
Cu-Zn	76.3	-	20.7	2.9	-	<1	-
Cu-Ni	66	30.4	-	2.6	< 1	-	<1

Figure 1 shows X-ray diffraction (XRD) patterns of the copper alloys used for this study. The crystallographic analysis confirmed unambiguously the characteristic lines of only the α-phase for both Cu-Zn and Cu-Ni alloys **[22]**. The diffraction peaks of the samples are indexed to cubic crystal structure of CuNi with space group Fm-3m (JCPDS Card No: 03-065-7246). Indeed, for Cu alloy with a copper content higher than 63 %, alloy has single phased micro structure with α-crystals only.

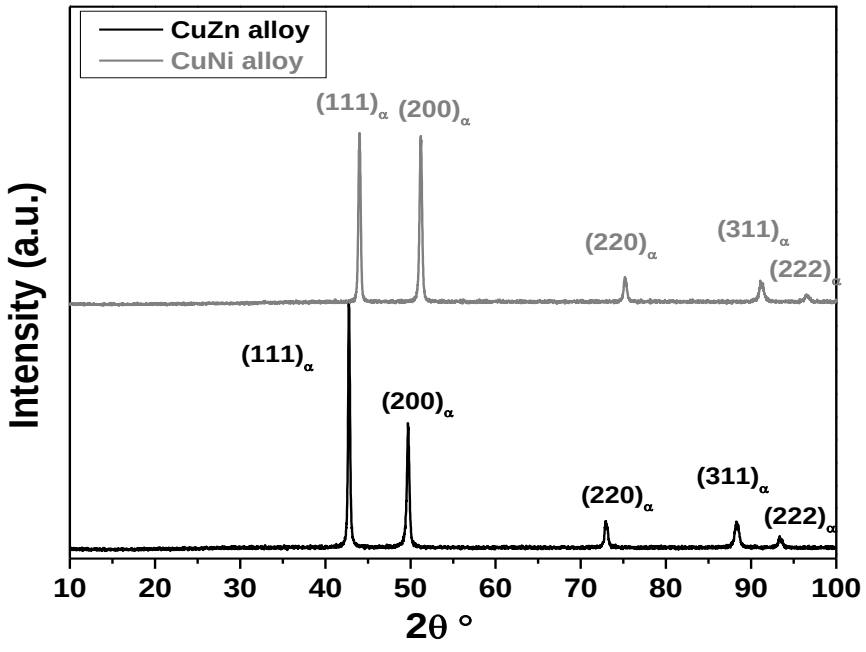

Figure 1: X-ray diffractograms of the Cu-Ni and Cu-Zn alloys surface before corrosion

Corrosion experiments

The copper alloys coupons were immersed in100 ml of 3% NaCl in static mode for 15, 30, 60 and 90 daysat room temperature. Thechoice of 90 days is motivated bymonitoring thestability of the filmformedonthecopper alloys surface as described intheliterature **[23].** According to the ASTM standard method for corrosion measurement (ASTM, 1966), the alloys coupons were then cleaned with HCl (15%) and sodium carbonate (5%) andfinally driedbyaforced airflow before experiments.

Electrochemical analysis

The electrolytic medium employed for the electrochemical tests is a 3% NaCl solution to simulate the sea water. The solution was obtained by dissolving 30 g of sodium chloride crystalline powder in 1L of distilled water and then stirred by a magnetic bar to have a homogeneous solution. The pH of the resulting solution was approximately neutral.

The electrochemical studies were carried out using potentiostat/galvanostat (model PGZ 301). Acquisition and basic treatment of spectra have been made with the VoltaMaster 4 software connected to a thermostated double-walled electrochemical cell.

A conventional three-electrode electrochemical cell of 400 mL was used. The cell assembly consisted of a platinum foil as counter electrode (C_E), saturated calomel electrode (SCE) as reference electrode (R_E) and Brass or cupronickel as working electrode with an exposed surface area of 1 cm^2 embedded in a chemically inert resin.

We applied to the studied samples a cathodic potential of -500 mV/SCE immediately after the introduction of the solution. The application of a cathode potential prevents the alloys to be passivated before testing. The sample is kept at the cathodic state for quarter hour before each test; which allows having the same surface condition and then ensuring good reproducibility. Polarization curves were obtained in a scanning field (-1000 to 300) mV/SCE. The potential was incremented by 0.5 mV/s**.**

Weight loss measurements.

For all experiments, the corrosion rate was determined according to the ASTM standard method for corrosion measurement, the corrosion layer was pickled with HCl (15%) and isopropanol with 5mg/Lof hexamethylenetetramine to inhibit further corrosion **[24]**.

The corrosion rate can be calculated using the following formula:

$$\text{Corrosion rate (micron/year)}: \frac{3650 \text{ x weight loss (mg)}}{\text{Density (g/cm}^3\text{) x Area (cm}^2\text{) x Time (days)}} \quad \textbf{(1)}$$

With a density of 8,4 g/cm^3 for brass and 8,9 g/cm^3 for cupronickel.

Chemical and surface analysis

At the end of reaction time, 10 mL of the solution was syringe-filtered using 0.2 µm polypropylene filter (Whatman). The solution was then analysed by atomic absorption spectrophotometer (Shimadzu 6680) equipped with an atomizer driven by the software running on the double beam principle, which avoids suffering the lamp fluctuations. The problems inherent in the measurement of a signal will be detected first, and thereafter, we measure the concentrations of copper, nickel and zinc dissolved in 3% NaCl after immersion for various times.

The morphology and chemical composition of the corrosion products were investigated using an Energy Dispersive Spectroscopy (EDS) coupled to a Scanning Electron Microscope (SEM). The analyses were done under an accelerating voltage of 15 kV. The Si(Li) detector used was equipped with a thin beryllium window that allows to detect and quantify oxygen.

The characterization of both alloys surface was achieved by X-ray diffraction and micro-Raman analysis. Single crystal powder X-ray diffraction pattern was recorded at room temperature using a Siemens D500 diffractometer in a Bragg- Brentano geometry using Cu-Kα_1 radiations (λ_1 = 1.54051 as X-ray source (cold cathode Crookes tube)). This latter is generated by a 2200 W copper anode (from Siemens, KFL CU 2K model, maximum potential: 60 kV). The data were collected in the range 5° to 100° in 2θ with a 0.02° 2θ-step and a count time of 20s per step.

The thick layers of corrosion products have been characterised by Raman spectroscopy. Raman spectra were carried out on the surface of Brass and cupronickel couponscorrodedfor 90 days in 3% NaCl solution at free potential and under aerated conditions. The Raman experiments were performed at room temperature using a T64000 Jobin-Yvon/Horiba spectrometer equipped with a 600 lines/mm diffraction grating and a nitrogen cooled CCD detector. The Raman spectra were recorded under a microscope (Olympus Bx41) in the back scattering geometrywith a 100x objective focusing the 514 nm line from an Argon–Krypton ion laser (coherent, Innova).The spot size of the laser was estimated at 0.8 µm and the spectral resolution at 2 cm^{-1}. Single spectra were recorded twice in the wavenumber 80-2000 cm^{-1} region with an integration time of 600 s. Acquisition and basic treatment of spectra have been made with the LabSpec V5.25 (Jobin Yvon-Horiba) software. Raman measurements were carried outat verylow laser powerto minimize possible sample deterioration or phase transition with operating time.

RESULTS AND DISCUSSION

Electrochemical study

Figure 2 shows the potentiokinetic polarization curves of Brass and cupronickel in 3% NaCl solution. The extent of the passivation level was determined by the difference between the zero-current potential ($E_{i=0}$) obtained from the straight line of Taffel and pitting potential (E_{pit}.).

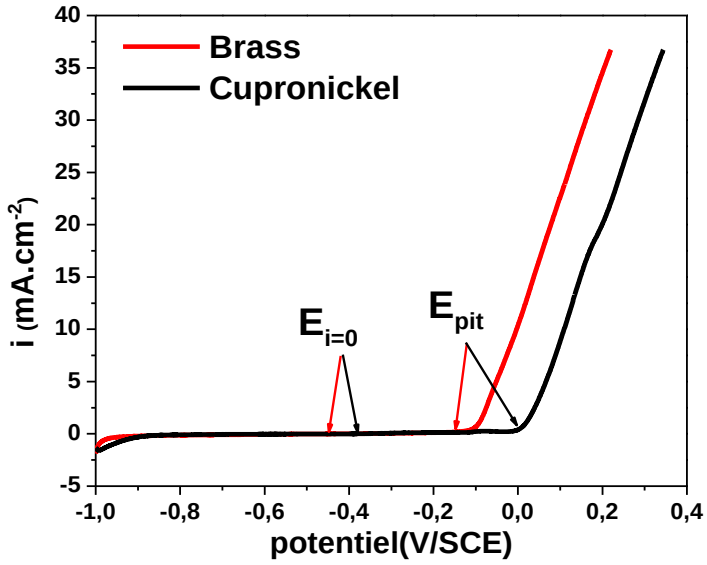

Figure 2: Potentiokinetic polarization curves (i-E) of Brass and cupronickel in3% NaCl solution

In **Figure 2**, we can distinguish the appearance of two zones. These zones can be described as follow:

• A cathodic zone, which extends from the starting potential (-1000 mV/SCE) to the zero current potential ($E_{i=0}$). In this region, we attend the reaction of oxygen reduction **[25]**:

$O_2 + H_2O + 4e^- \rightarrow 4OH^-$(2)

• An anode zone, where the polarization curves are composed of two areas. The first is between the corrosion potential ($E_{i=0}$) and pitting potential (E_{pit}) which defines the passivation area, demonstrating the formation of a protective film of which the current density is almost zero. The second area corresponds to the rupture zone of the passive film previously formed by the corrosion products on the alloys surface. The pitting of the film would be attributed to chloride ions **[26]**. Moreover, there is a sudden increase in current density which results in the attack of the alloys by pitting. This pitting makes the metal surface directly exposed to the electrolyte and leading to migration of metallic ions into the solution.

As seen in **Figure 2**, is clear that both binary alloys have a passivation level characterized by a zero-current potential ($E_{i=0}$) and a pitting potential (E_{pit}). However, we note that cupronickel is more resistant toward corrosion than brass ($E_{i=0}$ and E_{pit}, are more noble for cupronickel) whose values are respectively: (-0.389 V/SCE and 0.006 V/SCE) and (-0.441 V/SCE and -0.167 V/SCE).

In order to understand the behavior of the two alloys, we study the evolution of the passive film versus time using the polarization curves. Immersion periods used for this study are: 15, 30, 60 and 90 days.

Figure 3 illustrates the polarization curves of brass and cupronickel in 3% NaCl solution for various immersion times. The values of the zero-current potential ($E_{i=0}$) and the pitting potential (E_{pit}) corresponding are summarized in **Table 2**.

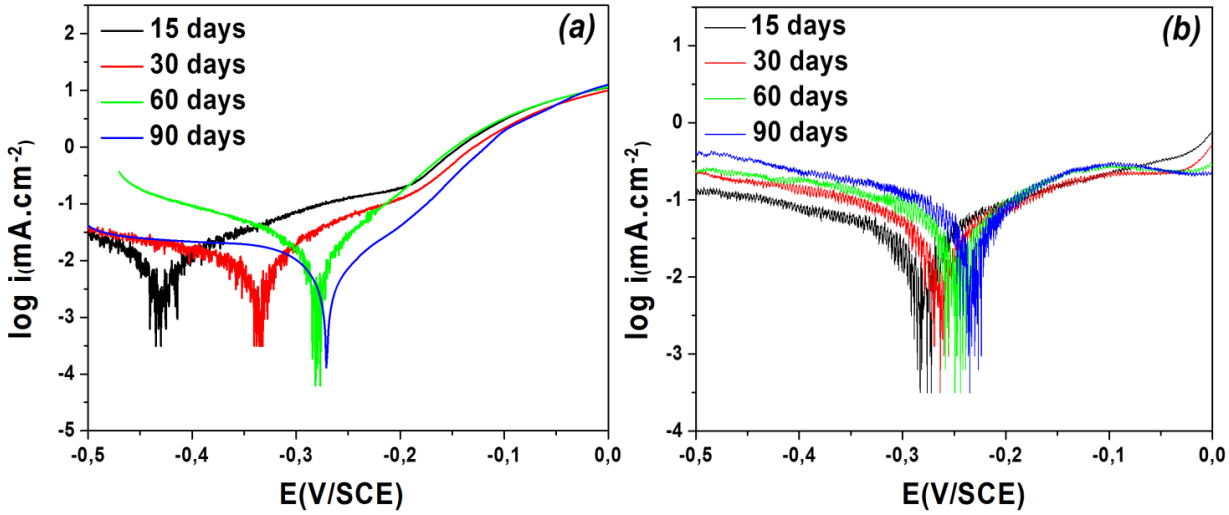

Figure 3: Evolution of polarization (log I = f (E) of alloys in 3% NaCl solution as a function of time immersion: (a) brass (b) cupronickel

Table 2: Values of zero-current and pitting potentials in the CuZn and CuNi alloys as afunction of time immersion

Immersion time **(jours)**	Brass			Cupronickel		
	$E_{i=0}$ (V/SCE)	E_{pit} (V/SCE)	$E_{pit}.E_{i=0}$ (V/SCE)	$E_{i=0}$ (V/SCE)	E_{pit} (V/SCE)	$E_{pit}.E_{i=0}$ (V/SCE)
15	-0.422	-0.170	0.252	-0.279	0.007	0.286
30	-0.333	-0.160	0.173	-0.264	0.010	0.274
60	-0.283	-0.170	0.113	-0.247	0.020	0.267
90	-0.270	-0.125	0.145	-0.233	0.031	0.264

Figure 3 shows a positive trend in zero-current potential as a function of immersion time for both alloys. After 90 days of immersion, the values obtained are -0.270 V/SCE for brass and -0.233 V/ SCE) for cupronnickel. The same observation is true for pitting potential.

The potential values ($E_{i=0}$ and E_{pit}) show the progressive formation of the passivation film as a function of time (**Table 2**).

In the early time of immersion (**Figure 3a and 3b**), the analysis show the presence of dissolution attack of alloys surface, which result in the cations transfert from metal into solution. However, when the corrosion layer was formed and becomes more stable and increasingly resistant with time immersion; this will limit the current flow at the material-electrolyte interface.

The formed film is probably consisting of adsorbed species, such as copper oxide (Cu_2O and CuO) for both alloys, nickel oxide NiO for cupronickel and ZnO for brass with a inhibitroy effect **[30-33]**.

We can deduce that brass and cupronickel have a similar electrochemical behavior. However, the study conducted on these materials showed that brass is less resistant in NaCl environment than the cupronickel. The low resistance of brass against corrosion by pitting is probably due to a formation of ZnO in the passive layer **[26-29].**

The results obtained by the electrochemical method were corroborated by the physicochemical study (analysis of the solution and structural characterization of the alloys surface).

Solution analysis

The solutions were analyzed by atomic absorption spectrophotometery to determine the concentration of Cu, Ni and Zn leached from the submerged samples. The numerical values of weight loss (NL) measured after each time aging and the factor corresponding to dezincification (DZ) and denickelfication (DN) factors are presented in **Table 3**.

The(DZ) and (DN) factors were calculated usingthe following formulas [**34]:**

$$DZ = \frac{\left(\frac{Zn}{Cu}\right)_{Sol}}{\left(\frac{Zn}{Cu}\right)_{all}} \quad \textbf{(3)}$$

$$DN = \frac{\left(\frac{Ni}{Cu}\right)_{Sol}}{\left(\frac{Ni}{Cu}\right)_{all}} \quad \textbf{(4)}$$

Where: $(Zn/Cu)_{sol}$: the concentration ratio of Zn/Cu in solution, $(Zn/Cu)_{all}$: the ratio of Zn/Cu in the alloy (% weight), $(Ni/Cu)_{sol}$: the concentration ratio of Ni/Cu in solution and $(Ni/Cu)_{all}$: the ratio of Ni/Cu in the alloy (% weight).

Table 3: Results of the solution analysisby atomic absorption spectrophotometery for copper alloys in 3% NaCl solution

Time aging (days)	Cu-Znalloy			Cu-Nialloy		
	Cu (g/m^2)	Zn (g/m^2)	DZ	Cu (g/m^2)	Ni (g/m^2)	DN
15	1.046	6.973	25.20	0.560	0.118	0.474
30	1.064	5.320	18.90	1.401	0.295	0.473
60	1.857	3.714	7.56	1.542	0.324	0.472
90	1.902	2.113	4.20	1.823	0.384	0.474

The analysis of the solutions after immersion of two alloys, revealed the presence of copper and zinc for brass and the presence of copper and nickel for the cupronickel. For brass, the zinc element is preferentially released compared to copper. The zinc concentrations in solution are more important than those of copper during the tests. We emphasize that the dezincification factor decreased with increasing immersion time: from a rate of 25.2 within the first 10 days to 4.2 after 90 days. The immersion of the brass in 3% NaCl solution results in the dezincification. Indeed, Brass is subject to selective corrosion, and the zinc which possesses a more negative standard potential compared to Cu is preferentially leached out of the brass leaving behind a brass matrix enriched in Cu.

The continuous dissolution results in the formation of a film composed of oxides of ZnO and Cu_2O [**35-37**], which lead with time immersion to a slowdown of the selective dissolution of zinc, due to a formation of protective layer on brass surface.

In the case of cupronickel, we can show the absence of competitiveness between the elements constituting the alloy. The dissolution of copper is accompanied by that of nickel. Moreover, there is a consistency of denickelfication factor. Unlike with the brass, in the case of Cu-Ni alloys, the nickel is retained in the oxide layer, and the presence of copper-nickel oxide prevents further nickel dissolution.

The pH of the solution before and after sample immersion remained stable, around 6.9 for Cu-Ni and 7.3 for Cu-Zn alloy. This indicates that the pH does not play a significant role on the corrosion kinetics.

During the previous section, we highlighted by electrochemical techniques, the formation of a passive film on both brass and cupronickel in 3% NaCl solution after 90 days. However, the precise identification of the corrosion products requires the use of other complementary surface analysis tools such as SEM and Raman spectroscopy.

Weight Loss and Corrosion Rate

The corrosion rate calculated from weight loss after 90 days of immersion in 3% NaCl solution are 41.9 µm/year for brass and 13.9 µm/year for cupronickel. This result confirmed that the brass is less resistant to corrosion in NaCl environment compared to cupronickel. The high corrosion rate observed can be attributed to a high dissolution of zinc.

The low corrosion rate for cupronickel is probably due to a formation of a thin protective layer which protect the alloy from further corrosion.

SEM analysis

Figure 4 shows the scanning electron micrographs of Cu-Zn and Cu-Ni alloys before and after 90 days of corrosion testing in 3% NaCl solution.

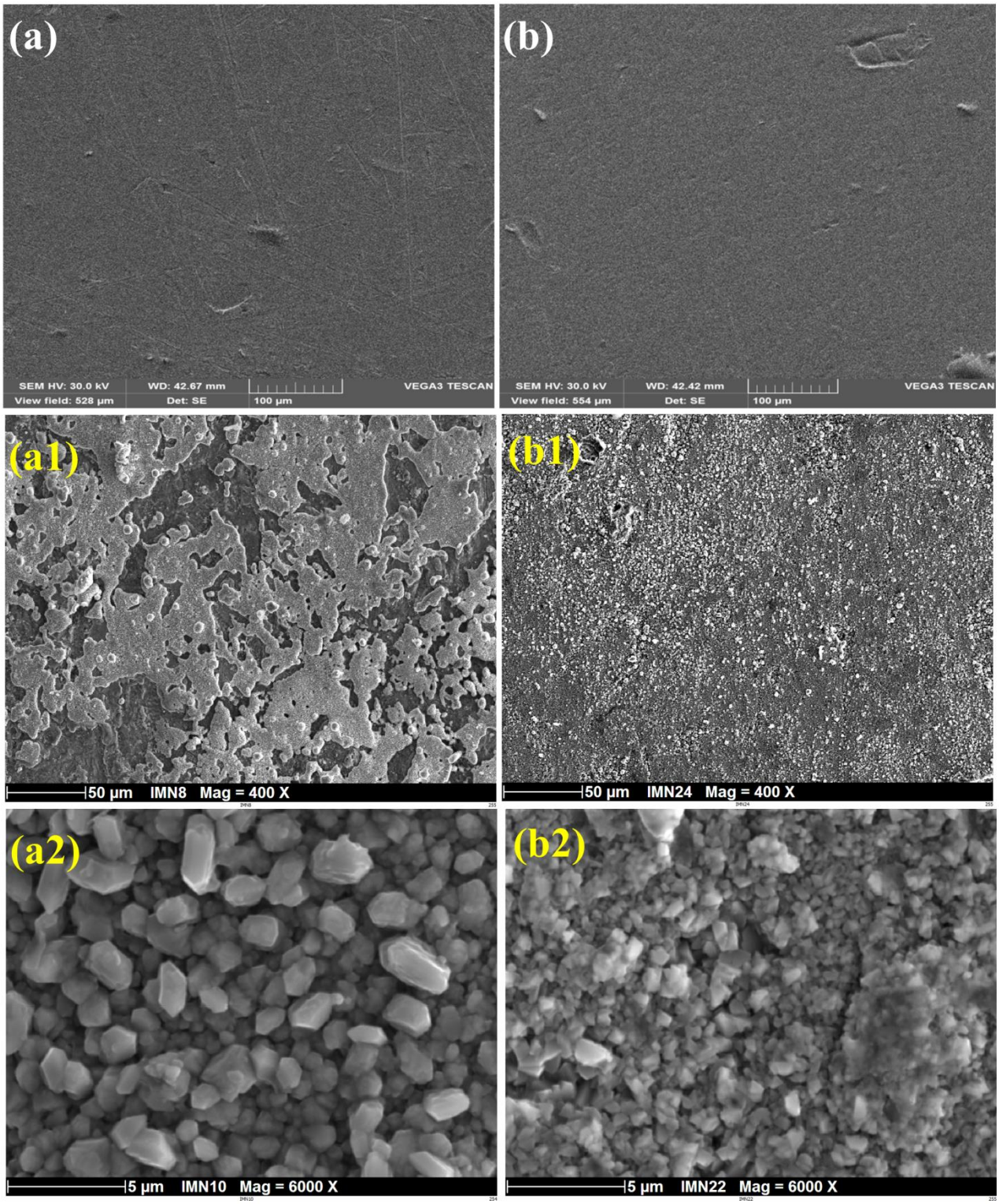

Figure 4 : SEM photographs of Cu-Zn and Cu-Ni alloys; (a) & (b) represent the uncorroded Cu-Zn and Cu-Ni, respectively; (a1, a2) & (b1, b2) represent the corroded Cu-Zn and Cu-Ni in 3% NaCl solution after 90 days, respectively

These SEM photographs show the development of a corrosion layer on the surface of Cu-Zn and Cu-Ni (**Figure 4-a1 and b1)** after 90 days. The layer formed on the Cu-Zn alloy exhibits intergranular corrosion (**Figure 4-a2**). This layer enriched in copper corrosion products due to the de-alloying of zinc. It was reported previously that ZnO is also more soluble than Cu_2O in chloride media and hence dezincification is predicted **[38]**. The precipitation of zinc corrosion products as ZnO as well as the copper corrosion products (such as Cu_2O and CuO) leads eventually to

limit the selective dissolution of zinc for a long immersion time by covering the maximum of brass surface. The difference in brightness observed on the image indicates that the layer formed after 90 days of time aging is not uniform. This phenomenon is related to a dezincification of Zn **[38]**.

The layer formed on the Cu-Ni alloy surface is dark green (CuO_2) with shiny grains (NiO) uniformly distributed over the surface of the alloy. These grains are less dense than those observed in the case of the Cu-Zn alloy (**Figure 4-b2**). This clearly indicates the mutual contribution of the two oxides (Cu_2O and NiO) in the film (low preferential dissolution of nickel) as has been shown in the electrochemical study.

The EDX spectra of the corroded surface are shown in **Figure 5**. The EDX analysis of the oxide film formed on the Cu-Zn alloy reveals the presence of oxygen, copper and zinc, oxygen and chloride. For the case of Cu-Ni alloy, the analysis of the oxide film revealed the presence of copper and nickel, oxygen and chloride.

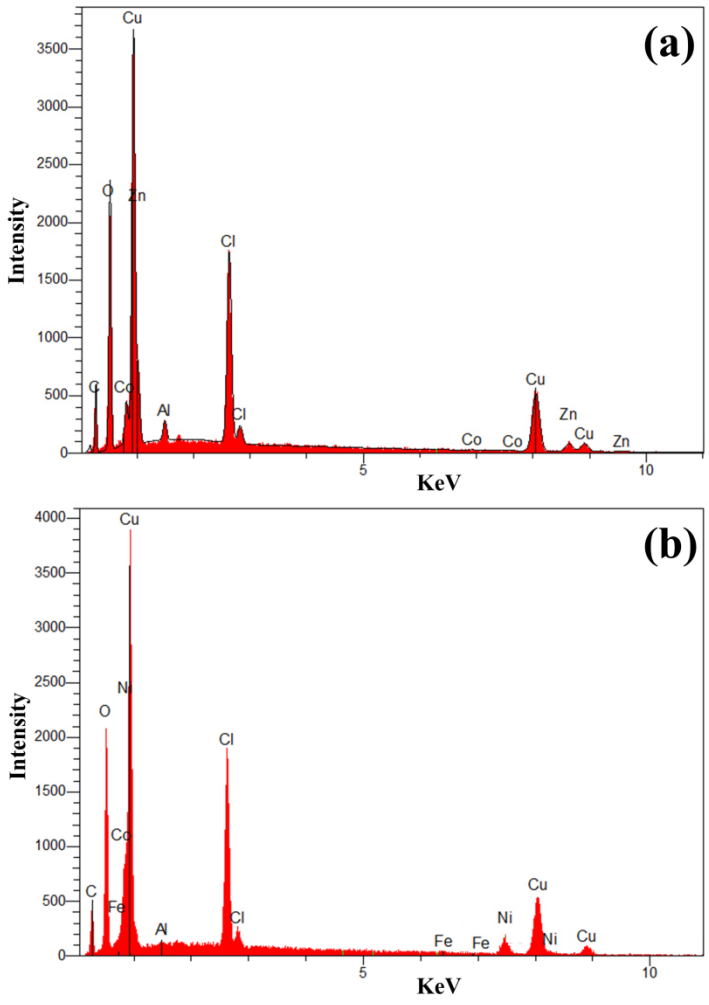

Figure 5:EDX spectra of corroded surface: (a) Cu-Zn alloy surface (figure4-a1) and (b): Cu-Ni alloy surface (figure 4-b1)

The composition of the corrosion layer formed on surface in both alloys is summarized in **Table 4.**

Table 4: Thecomposition of thecorrosion layer formed on surface in both alloys

Elements	Cu-Znalloy		Cu-Nialloy	
	Before corrosion	After corrosion	Before corrosion	After corrosion
Cu	76.3	25.7	66.0	31.4
Zn	20.7	4.5	-	-
Ni	-	-	30.4	10.7
Cl	-	14.2	-	14.9
O	-	43.4	-	42.5
Al	2.9	2.0	2.6	<1
Co	<1	-	-	-
Fe	-	-	<1	<1
Mn	-	-	<1	<1

The corrosion layer formed on brass surface is enriched in copper corrosion products due to the rapid de-alloying of zinc, while for the cupronickel; the corrosion layer enriched in copper and nickel corrosion products. These results are in agreement with solution data. Indeed nickel is retained in the oxide layer, and the formation of Cu-Ni oxide prevents further denickelfication of cupronickel.

The EDX analysis indicates that the layer is composed of a mixture of copper, nickel, chlorine and oxygen for Cu-Ni alloy (copper, zinc, chlorine and oxygen for brass), but it was not possible to determine the composition of the oxide. For this purpose we used Raman spectroscopy for the surface microanalysis.

Raman analysis

The Raman spectra of the brass coupon surface (**Figure 6**) show the presence of the vibration mode of the crystalline Cu_2O **[39]**. Indeed, for Cu_2O, five distinct bands located at 113, 147, 215, 415 and 635 cm^{-1} are expected. In addition, the weak peaks observed at 308 and 515 cm^{-1} are commonly assigned to the second-order modes of Cu_2O. The Raman investigations reveal also the presence of the ZnO characterized by the intense vibration mode E_2 at 436 cm^{-1}. The low intensity peaks were observed at 330, 516, 576, and 650 cm^{-1}. The peaks at 330, 516, and 650 cm^{-1} are directly associated with the vibration mode caused by multiple-phonon scattering processes **[40]** and the peak at 576 cm^{-1} corresponds to the LO phonon of the A_1 mode.

The Raman spectrum of CuO shows very sharp peaks around 296, 345 and 627 cm^{-1}. The former peak at 296 cm cm^{-1} belongs to A_g mode where as two latter peaks at 345 and 627 cm^{-1} are assigned to B_g modes of CuO, respectively which are in good agreement with the previously reported data **[41]**.

In addition, the Raman analysis confirmed the presence of the bands at 120, 145, 365, 509 and 940cm^{-1} typical of kapellasite ($Cu_3Zn(OH)_6Cl_2$) **[42]**,which is the metastable polymorph of herbertsmithite. According to the litterature **[43]**, Kapellasite can be synthesized from $ZnCl_2$ solution and metallic copper metal. The observation by optical microscopy confirmed the green color of Kapellasite. A series of minerals related to the $Cu_2(OH)_3Cl$ polymorphs are characterized by solid-solution phenomena in the group. Substitution for Cu^{2+} is known to occur commonly with divalent Zn, Ni, Co, Mn, Fe and Mg ions **[44]**.

For the cupronickel, our investigations show similar spectra for Cu_2O. However, Raman measurements reveal the presence of NiO and gillardite(($Cu_3Ni(OH)_6Cl_2$), which is also isostructural with herbertsmithite. The spectrum for gillardite appears similar to that of herbertsmithite measured by Wulferding *et al*. **[45]** and in this study. The frequency shift of related modes between girraldite and herbertsmithite could be due to solid solution effects caused by the difference in crystal-chemical behaviour of Ni^{2+} and Zn^{2+} **[45,46]**.

For NiO: there are five vibrational bands – one - phonon (1P) TO at 440 cm^{-1} and LO at 560 cm^{-1} modes, two-phonon (2P) 2TO at 740 cm^{-1} and TO+LO at 925 cm^{-1} **[47]**.

The presence of Kapellasiteand gillardite clearly showsinteractions betweenchlorine originating from the medium and the alloys, as indicated by the presence of Zn^{2+} (or Ni^{2+}) and Cu^{2+} in solution (atomic absorption spectrophotometery analysis). The formation of Kapellasite (or gillardite) may be due to chemical reactions involving the chloride complexes $ZnCl_2$ (or $NiCl_2$) and $Cu(OH)_2$, according to the reactions:

$$\mathbf{3Cu(OH)_2 + Zn^{2+} + 2Cl^- \rightarrow Cu_3Zn(OH)_6Cl_2} \quad \textbf{(5)}$$

$$\mathbf{3Cu(OH)_2 + Ni^{2+} + 2Cl^- \rightarrow Cu_3Ni(OH)_6Cl_2} \quad \textbf{(6)}$$

For cupronickel, the spectral features of CuO are somewhat different to those found on the brass surface but appear very similar to those reported in a recent study by Chand et al. **[48]**. These authors report the effect of Ni doping on the structural and optical properties of CuO nanocrystals at different concentrations of Ni^{+2} ions ($Cu_{1-x}Ni_xO$ with x = 0.0, 0.05, 0.10, 0.15 and 0.20). Our spectrum is close to that obtained by theses authors for $Cu_{1-x}Ni_xO$ nanostructures with x = 0.15, with the presence of a shoulder band at 275 cm^{-1} in addition to a broadening of the Raman modes. The broadening and downshifts of the Raman peaks are mainly attributed to the quantum confinement effect of CuO nanostructures.

This result is in good agreement with the EDX analysis (**Figure 5**). Indeed, the compositions of the layer formed on the cupronickel surface shows that the corrosion products are enriched in Ni.

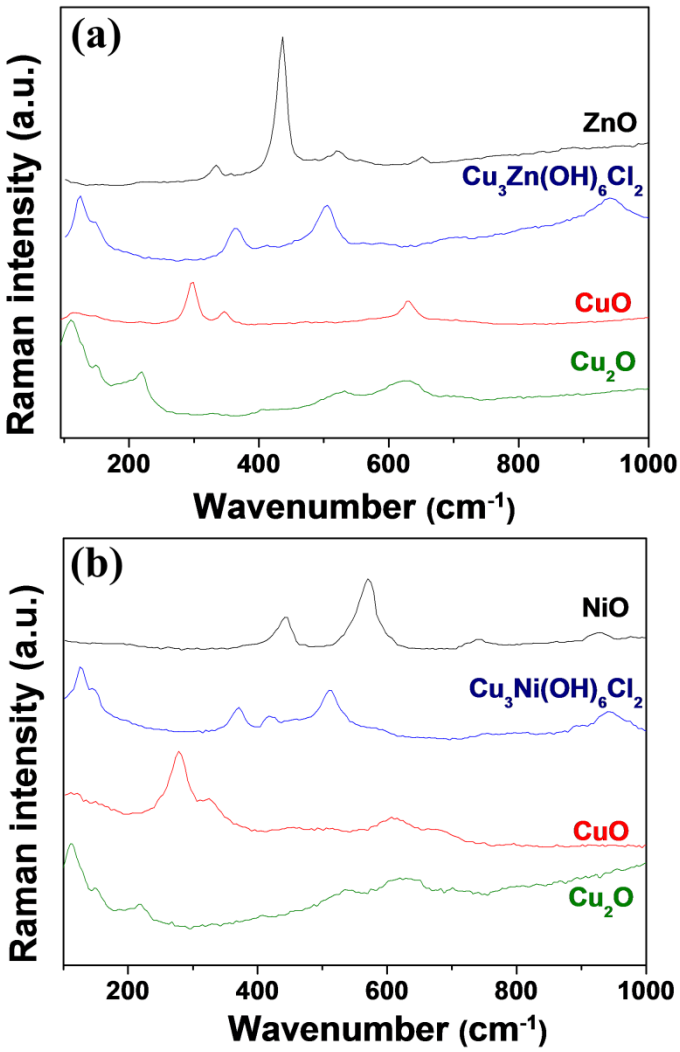

Figure 6: Raman spectraof the corrosion products formedon the Brass surfaceafter 90 days in 3% NaCl solution (a) Cu-Zn alloy, (b) Cu-Ni alloy

North and Pryor explained the resistant towards corrosion of the copper–nickel alloy in terms of the defective semi-conductor property of the Cu_2O film on the copper-base alloys **[49]**; this is the case for CuO that is a material with semiconducting properties. These authors hypothesized that nickel were incorporated into the Cu_2O film, occupied cation vacancies, and reduced the ionic or electronic conductivity of the film, improving the corrosion resistance. This statement has been adopted subsequently by different authors to explain corrosion resistance of copper–nickel alloys in chloride solutions by electrochemical techniques **[50-53]**.

In the absence of Raman study on of CuO_2 doped with nickel, we cannot confirm the assumptions of North and Prior **[50]**, but it seems that in our study, this is the case for CuO.

CONCLUSION

In summary, it has been demonstrated by electrochemicalmeasurements that Cu-Ni is much more resistant to chloride aggressive environment than Cu-Zn. The weight loss measurements shows that the corrosion rate after 90 days are 41.9 µm/year for brass and 13.9 µm/year for cupronickel. The structural caracterisation by SEM/EDX and Ramanspectroscopy shows results in good agreement with the electrochemical data and thus confirmed the difference in the brass and cupronickel surface composition after 90 days.The formedfilm on the cupronickel is characterized by the presence of nickel in the corrosion produts, which leads to a film passivity and reduces the denickelfication of cupronickel. Hence, cupronickel apperas to be the most beneficial solution for sea water desalination installations.

Acknowledgements
Special thanks to N. Stephant (Institut des Matériaux de Nantes, CNRS/université de Nantes) for the SEM-EDX measurements.

REFERENCES

[1] M. M. Antonijevic; M. B. Petrovic, *Int. J. Electrochem. Sci.*, **2008**, 3, 1-28
[2] C Deslouis; G Mengoli; B Tribollet, *J. Appl. Electrochem. Soc.* **1983**, 130(10), 2044-2046
[3] H Lu, K Gao; W Chu, *Corros. Sci.*, **1998**, 40(10), 1663-1670.
[4] VK Gouda; IZ Selim; AA Khedr; AM Fathi, *J. Mater. Sci. Technol.*, **1999**, 15, 208.
[5] J Morales; GT Fernandez; P Esparza; S Gonzalez; RC Salvarezza; AJ Arvia, *Corros. Sci.*, **1995**, 37, 211-225.
[6] AM Beccaria; ED Mor; G Poggi; F Mazza, *Corros. Sci.*, **1987**, 27, 363-372.
[7] HG Bachmann, The identification of slags from archaeological sites, published by the Institute of Archaeology of London, Occasional Publication No. 6, Institute of Archaeology, London, **1982**.
[8] A Giumlia-Mair, Revue De Métallurgie, **2001**, 98(9), 767-776.
[9] R Procaccini; WH Schreiner; M Vazquez; S Ceré, *Appl. Surf. Sci.*, **2013**, 268, 171-178.
[10] J Kunze; V Maurice; LH Klein; HH Strehblow; P Marcus, *Corros. Sci.*, **2004**, 46, 245-264.
[11] G Kear; BD Barker; FC Walsh, *Corros. Sci.*, **2004**, 46, 109-135.
[12] TK Mikic; I Milosev; B Pihlar, *J. Appl. Electrochem.*, **2005**, 35, 975-984.
[13] J Morales; GT Fernandez; P Esparza; S Gonzalez; RC Salvarezza; AJ Arvia, *Corros. Sci.*, **1995**, 37, 211-229.
[14] KM Ismail; RM Elsherif; WA Badawy, *Electrochim. Acta.*, **2004**, 49, 5151-5160.
[15] Z Avramovic; M Antonijevic, *Corros. Sci.*, **2004**, 46, 2793-2802.
[16] S maroie; R Caudano; G debras; J Verbist, Appl. Surf. Sci., 1980, 4, 466-480.
[17] R Procaccini; M Vazquez; S Cere, *Electrochim. Acta.*, **2009**, 54, 7324-7329.
[18] J Morales; GT Fernandez; P Esparza; S Gonzalez; RC Salvarezza; AJ Arvia, *Corros. Sci.*, **1998**, 40, 177-190.
[19] L Burzynska; A Maraszewska; Z Zembura, *Corros. Sci*., **1996**, 38, 337-347.
[20] JY Zou; DH Wang; WC Qiu, *Electrochim. Acta.*, **1997**, 43, 1733-1737.
[21] M Metikoš-Huković; R Babić; I Škugor Rončević; Z Grubač, *Desalination*, **2011**, 276, 228-232.
[22] F El-Chiekh; MT El-Haty; H. Minoura; AA Montaser, *Electrochim. Acta.*, **2005**, 50, 2857-2864
[23] AH Tuthill, Guidelines for the use of Copper alloys in Seawater, Materials performances, September **1987**.
[24] Y El Mendili; A Abdelouas; JF Bardeau, *J. Mater. Environ. Sci*., **2013**, 4, 786-791.
[25] HG Jiang; M Ruhle; EJ Lavernia. *J. Mater. res.*, **1999**, 14, 549-559.
[26] SAM Refaey, *Appl. Surf. Sci.*, **2000**, 158, 190-196.
[27] MV Rylkina; YI Kuznetsov; MV Kalashnikova; MA Eremina, *Protect. Met.*, **2002**, 38, 387-393.
[28] MB Valcarce; SR de Sanchez; M Vazquez, *Corros. Sci*., **2005**, 47, 795-809.
[29] T Kosec; I Milosev; B Pihlar, *Appl. Surf. Sci.*, **2007**, 253, 8863-8873.
[30] YZ Wang; AM Beccaria; G Poggi, *Corros. Sci.*, **1996**, 38, 835-851.
[31] RF North; MJ pryor, *Corros. Sci.*, **1970**, 10, 297-311.
[32] C Kato; BG Ateya; JE Castele; HW pickering, *J. Electrochem. Soc.*, **1980**, 127, 1890-1896.
[33] G Kear; BD Barker; K Stockes; FC Walsh, *J. Appl. Electrochem.*, **2004**, 34, 659-669.
[34] G Trabanali, A Garassiti, Advance in Corrosion Science and Technology, Plenum Press, New York, **1970**.
[35] FM Al-Kharafi; YA El-Tatawy, *Corros. Sci.*, **1982**, 22, 1-12.
[36] Z Xia; Z Szklarska-smialowska, *Corrosion.*, **1990**, 46, 85-88.
[37] AA El Warraky, *Br. Corros. J.*, **1997**, 32, 57-61.
[38] O Fruhwirth; GW Herzog; J Poulios, *Surf. Technol*., **1985**, 24, 293-300.
[39] A. Compaan; H. Z. Cummins, *Phys. Rev. B.*, **1972**, 6, 4753-4757.
[40] N Ashkenov; BN Mbenkum; C Bundesmann; V Riede; M Lorenz; D Spemann; EM Kaidashev; A Kasic; M Schuber; M Grundmann; G Wagner; H Neumann; V Darakchieva; H Arwin; B Monemar, *J. Appl. Phys.*, **2003**, 93, 126-133.
[41] T Yu; X Zhao; Z X Shen; YH Wu; WH Su, *J. Crystal Growth.*, **2004**, 268, 590-595.
[42] GG Rotondo; L Darchuk; M Swaenen; R Van Grieken, *J. Anal. Sci. Method. Instrum.*, **2012**, 2, 42-47
[44] JL Jambor; JE Dutrizac; AC Roberts; JD Grice; JT Szymański, *Canad. Mineral.*, **1996**, 34, 61-72.
[45] D Wulferding; P Lemmens; P Scheib; J Röder; P Mendels; S Chu; T Han; YS Lee, *Phys. Rev.*, **2010**, B 52, 144412.
[46] RL Frost; W Martens; JT Kloprogge; PA Williams, *J. Raman. Spectrosc.*, **2002**, 33, 807-806.
[47] E Cazzanelli; A Kuzmin; G Mariotto; N Mironova-Ulmane, *J. Phys.: Cond. Matter.*, **2003**, 15, 2045-2052.
[48] P Chand; A Gaur; A Kumar, *Appl. Sci. Lett.*, **2015**, 1(1), 28-32
[49] RF North; MJ Pryor, *Corros. Sci.*, **1970**, 10, 297-311.
[50] SJ Yuan; SO Pehkonen, *Corros. Sci.*, **2007**, 49, 1276-1304.
[51] I Milosev; M Metikos-Hukovic, *Electrochim. Acta.* **1997**, 42, 1537-1548.

[52] M Metikoš-Hukovic; R Babic; I Škugor; Z Grubac, *Corros. Sci.*, **2011**, 53, 347-352.
[53] G Kear; BD Barker; K Stokes; FC Walsh, *J. Appl. Electrochem.*, **2004**, 34, 659-669.